JOM 23086

Photochemical reactivity of $[Ru^{II}(L)(CO)_2Cl_2]$ and $[Me_4N]$ $[Ru^{II}(L)(CO)Cl_3]$ (L = 2,2′-bipyridine or 4,4′-di(isopropoxycarbonyl)-2,2′-bipyridine) in CH_3CN and the redox properties of the resulting new complexes

Marie-Noëlle Collomb-Dunand-Sauthier and Alain Deronzier

Laboratoire d'Electrochimie Organique et de Photochimie Rédox (URA CNRS 1210), Université Joseph Fourier Grenoble 1, BP 53X, 38041 Grenoble Cédex (France)

Raymond Ziessel

Ecole Européenne des Hautes Etudes des Industries Chimiques de Strasbourg, Institut de Physique et de Chimie des Matériaux, Groupe des Matériaux Inorganiques, URM CNRS 46, 1 rue Blaise Pascal, BP 296F, 67008 Strasbourg Cédex (France)

(Received May 21, 1992)

Abstract

Photolysis of acetonitrile solutions of $[Ru^{II}(L)(CO)_2Cl_2]$ or $[Me_4N][Ru^{II}(L)(CO)Cl_3]$ (L = 2,2′-bipyridine or 4,4′-di(isopropoxycarbonyl-2,2′-bipyridine) leads to the successive formation of the new complexes $[Ru(L)(CO)(CH_3CN)Cl_2]$, $[Ru(L)(CH_3CN)_2Cl_2]$, and $[Ru(L)(CH_3CN)_3Cl]^+$ by photosubstitution processes. However, $[Ru(L)(CH_3CN)_2Cl_2]$, unlike $[Ru(L)(CO)(CH_3CN)Cl_2]$ and $[Ru(L)(CH_3CN)_3Cl]^+$, cannot be obtained quantitatively with the complex having the unsubstituted 2,2′-bipyridine ligand. Moreover $[Ru(L)(CH_3CN)_3Cl]^+$ cannot be produced at a significant rate for complexes with L = 4,4′-isopropoxycarbonyl-2,2′-bipyridine. The redox behaviour of all these compounds was studied by cyclic voltammetry at a platinum electrode, exhaustive electrolysis experiments, and UV-visible absorption spectroscopy.

1. Introduction

Polypyridyl complexes of ruthenium have been implicated as catalysts in the photo- and electro-chemical reduction of CO_2 [1]. $[Ru(bpy)(CO)_2Cl_2]$ (bpy = 2,2′-bipyridine) appears to be one of the most promising catalyst precursors [2–3]. However the identity of the catalytically active species remains unknown and little has been published concerning the redox and photochemical properties of this complex. It has been suggested that $[Ru(bpy)(CO)_2Cl_2]$, prepared from "ruthenium red carbonyl solution" [4], can be isolated as a red-purple compound, considered to be the *cis* isomer. This compound can be converted into a yellow complex (*trans* isomer) upon heating under reflux in water-ethanol solution [5]. We have recently demonstrated [6] that the yellow form is pure $[Ru^{II}(bpy)(CO)_2Cl_2]$ and that the red-purple form is a mixture of $[Ru^{II}(bpy)(CO)_2Cl_2]$ and $[Ru^{III}(bpy)(CO)Cl_3]$. The last, hitherto unreported, has been reduced electrochemically and isolated as $[Me_4N]$ $[Ru^{II}(bpy)(CO)Cl_3]$. We report here a detailed study of photo-induced ligand substitutions in both $[Ru^{II}(bpy)(CO)_2Cl_2]$ and $[Me_4N]$-$[Ru^{II}(bpy)(CO)Cl_3]$ under irradiation in CH_3CN. A similar study has been conducted with 4,4′-di(isopropoxycarbonyl)-2,2′-bipyridine in place of 2,2′-bipyridine. The electron-withdrawing ester groups stabilize the reduced forms, as observed, for instance, with some bipyridine complexes of rhenium(I) [7].

Correspondence to: Dr. A. Deronzier.

0022-328X/93/$6.00

2. Results and discussion

2.1. Photolysis of $[Ru(bpy)(CO)_2Cl_2]$

2.1.1. Formation of $[Ru(bpy)(CO)(CH_3CN)Cl_2]$

Selective irradiation of $[Ru(bpy)(CO)_2Cl_2]$ (1.1×10^{-3} M) in CH_3CN at 366 nm produces rapidly and exclusively $[Ru(bpy)(CO)(CH_3CN)Cl_2]$. Figure 1(A) illustrates the spectral changes during the photolysis. The successive UV-visible curves pass through an isosbestic point at 318 nm. The new species has an MLCT absorption band (λ_{max} (ϵ; 1 mol^{-1} cm^{-1}) = 460 nm (1.53×10^3), 341 nm, sh) which is shifted to the red compared to that of the initial complex (λ_{max} = 352 nm). This is consistent with carbonyl loss as previously reported for other ruthenium carbonyl complexes [8]. The quantum yield for the photosubstitution is close to unity. The identity of $[Ru(bpy)(CO)(CH_3CN)Cl_2]$ has been confirmed by IR spectroscopy (ν(CN) at 2274 cm^{-1}, only one CO band at 1965 cm^{-1}) and by fast atomic bombardment mass spectrometry, positive mode (FAB^+) (396.8 $[M+H]^+$, 361.9 $[M+H-Cl]$, 355.9 $[M+H-CH_3CN]$, 320.9 $[M+H-Cl-CH_3CN]$ *. The cyclic voltammogram (CV) in CH_3CN + 0.06 M TMATF (tetramethylammonium tetrafluoroborate) of the photolyzed solution shows a reversible $Ru^{2+/3+}$ system ($E_{1/2}$ = 0.75 V) in the anodic region at a less positive potential than that of the initial complex ($E_{1/2}$ = 1.45 V [6]) (Fig. 2, curves a and b). This change is in agreement with the poorer electron accepting ability of CH_3CN compared to CO. Exhaustive oxidation at 0.95 V requires one electron per molecule and leads to the stable Ru^{III} species $[Ru^{III}(bpy)(CO)(CH_3CN)Cl_2]^+$. The solution of the last exhibits absorption bands at 486 nm (1.52×10^3) and 406 nm (1.95×10^3) (Fig.

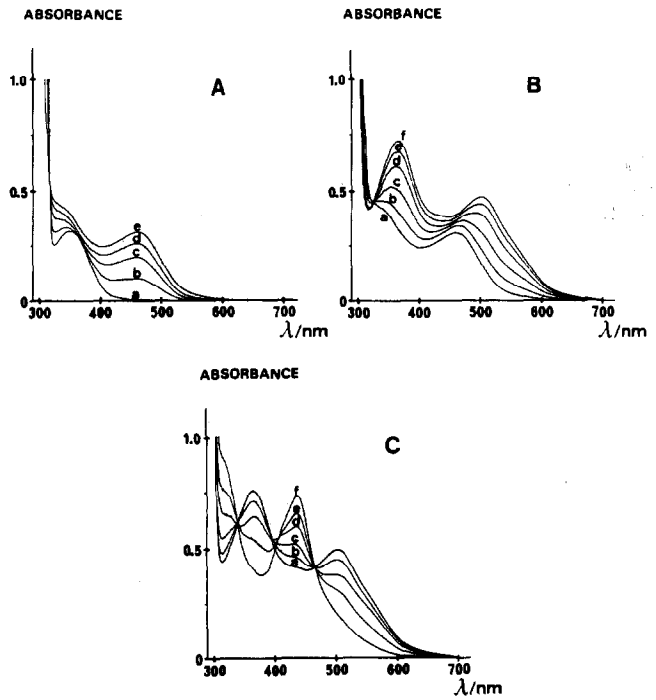

Fig. 1. Spectral changes during irradiation with a 250 W mercury lamp at 366 nm of a solution of $[Ru(bpy)(CO)_2Cl_2]$ 1.1 mM in CH_3CN. (A) Formation of $[Ru(bpy)(CO)(CH_3CN)Cl_2]$: (a) t = 0 s, (b) t = 30 s, (c) t = 1 min 30 s, (d) t = 2 min 30 s, (e) t = 4 min 30 s. (B) Formation of $[Ru(bpy)(CH_3CN)_2Cl_2]$: (a) t = 4 min 30 s, (b) t = 10 min, (c) t = 20 min, (d) t = 35 min, (e) t = 50 min, (f) t = 1 h 10 min. (C) Formation of $[Ru(bpy)(CH_3CN)_3Cl]^+$: (a) t = 1 h 30 min, (b) t = 2 h 10 min, (c) t = 3 h 10 min, (d) t = 4 h 25 min, (e) t = 6 h, (f) t = 11 h 10 min.

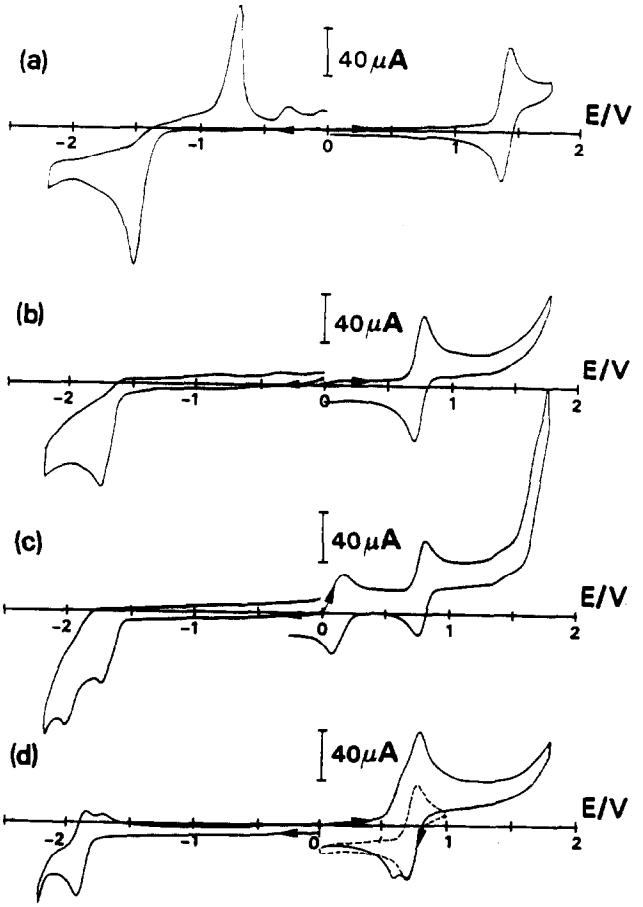

Fig. 2. Cyclic voltammograms at a Pt electrode (diameter 5 mm) in CH_3CN + 0.06 M TMATF; sweep rate ν = 100 mV s^{-1}. (a) solution of 1.05 mM $[Ru(bpy)(CO)_2Cl_2]$; (b) after formation of $[Ru(bpy)(CO)(CH_3CN)Cl_2]$ (1.05 mM); (c) after formation of $[Ru(bpy)(CH_3CN)_2Cl_2]$ (0.54 mM) + $[Ru(bpy)(CO)(CH_3CN)Cl_2]$ (0.66 mM) (see text); (d) after formation of $[Ru(bpy)(CH_3CN)_3Cl]^+$ (0.9 mM) (- - - - -) after oxidation at 0.9 V.

* All FAB^+ mass spectra described in this paper exhibit a molecular ion peak at the expected value with the correct isotopic distribution pattern (simulated by computer).

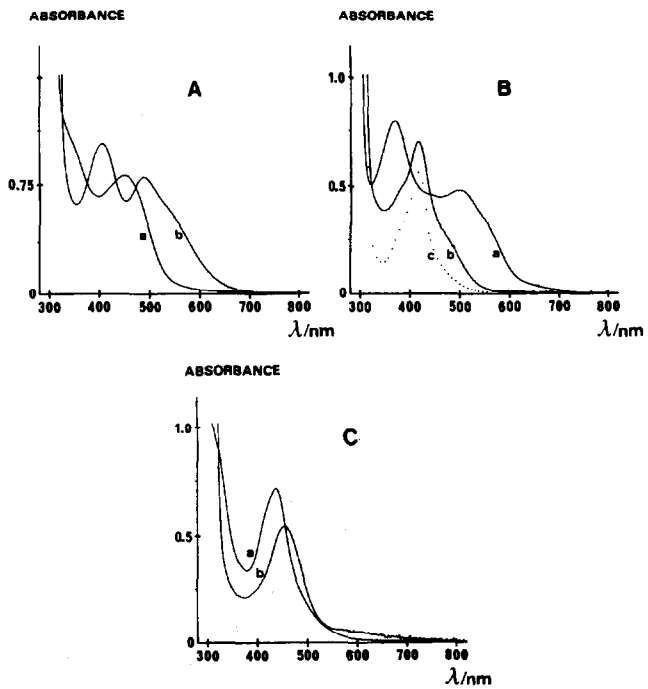

Fig. 3. Spectral changes during oxidation in CH_3CN+0.06 M TMATF of (A) a solution of $[Ru(bpy)(CO)(CH_3CN)Cl_2]$ 1.05 mM: (a) initial solution; (b) after oxidation at 0.95 V; Q = 1 electron per molecule. (B) a solution of $[Ru(bpy)(CH_3CN)_2Cl_2]$ (0.56 mM)+ $[Ru(bpy)(CO)(CH_3CN)Cl_2]$ (0.64 mM): (a) initial solution; (b) after oxidation at 0.4 V; Q = 1 electron per molecule; (c) corrected spectrum of $[Ru(bpy)(CH_3CN)_2Cl_2]$. (C) a solution of $[Ru(bpy)(CH_3CN)_3Cl]$ (0.9 mM): (a) initial solution; (b) after oxidation at 1.0 V; Q = 1 electron per molecule.

3(A)). After electrolysis the solution was evaporated to dryness and the complex extracted twice with CH_2Cl_2. The resulting solution free of TMATF was analyzed by FAB^+ and IR spectroscopy in order to confirm the photoinduced monosubstitution of CO by CH_3CN. There is only one CO band ($\nu(CO) = 1986\ cm^{-1}$, $\nu(CN) = 2297\ cm^{-1}$) and FAB^+ shows the $[Ru^{III}(bpy)(CO)(CH_3CN)Cl_2]^+$ molecular peak at 395.8 $[M^+]$, and a fragment at 360.8 [M–Cl]. In the cathodic region, the CV of $[Ru^{II}(bpy)(CO)(CH_3CN)Cl_2]$ has an irreversible peak at −1.75 V with no anodic peak in the reverse scan. Unlike with $[Ru(bpy)(CO)_2Cl_2]$ [6], no film or precipitate is formed on the working electrode during the exhaustive reduction. The resulting red-brownish solution does not exhibit any clear electrochemical response except that of the well-known quasi-reversible peaks of Cl^- [9] (Ep_a *ca.* 0.74 V) * released during the reduction step. This means that the reduction probably leads to decomposition.

* In fact the value of Ep_a is roughly dependent on the etching of the surface of the electrode.

2.1.2. Formation of $[Ru(bpy)(CH_3CN)_2Cl_2]$

After $[Ru(bpy)(CO)(CH_3CN)Cl_2]$ is formed, photolysis at 366 nm induces a slower modification of the absorption spectrum of the solution. Two new bands appear, at 502 and 366 nm (Fig. 1(B)). These new bands are attributed to a complex in which the two CO ligands are substituted by CH_3CN. The shift of the maximum of the absorption to higher wavelengths is in good agreement with this. However $[Ru(bpy)(CH_3CN)_2Cl_2]$ cannot be obtained quantitatively. After the band at 502 nm reached its maximum intensity, the CV showed a new reversible system at a less anodic potential ($E_{1/2} = 0.10$ V) with a large amount of residual mono-substituted complex $[Ru(bpy)(CO)(CH_3CN)Cl_2]$, as judged by the intensity of its reversible anodic system at $E_{1/2} = 0.75$ V (Fig. 2, curve c). Only 45% of the theoretical amount of $[Ru(bpy)(CH_3CN)_2Cl_2]$ can be produced in such a way.

The difference of potential between the $E_{1/2}$ of $[Ru(bpy)(CH_3CN)_2Cl_2]^{0/+}$ and $[Ru(bpy)(CO)(CH_3CN)Cl_2]^{0/+}$ ($\Delta E_{1/2} = 0.65$ V) is similar to that between the $E_{1/2}$ of $[Ru(bpy)(CO)(CH_3CN)Cl_2]^{0/+}$ and $[Ru(bpy)(CO)_2Cl_2]^{0/+}$ ($\Delta E_{1/2} = 0.70$ V), a consequence of the poorer electron-accepting capacity of CH_3CN compared to that of CO. Exhaustive electrolysis at 0.4 V furnishes the corresponding Ru^{III} species $[Ru^{III}(bpy)(CH_3CN)_2Cl_2]^+$. The absorption spectrum of this new complex can be deduced from the combined spectrum recorded after electrolysis, assuming that *ca.* 55% of $[Ru^{II}(bpy)(CO)(CH_3CN)Cl_2]$ is still present in solution. Figure 3(B), curve c, gives this calculated spectrum ($\lambda_{max} = 416$ nm) (5.54×10^3). In the cathodic region the voltammogram of the photolyzed solution (Fig. 2, curve c) exhibits two irreversible peaks. The first at $Ep_c = -1.75$ V is attributable to $[Ru(bpy)(CO)(CH_3CN)Cl_2]$ (see above). The second ($Ep_c = -2.03$ V) corresponds to the reduction of $[Ru(bpy)(CH_3CN)_2Cl_2]$.

2.1.3. Formation of $[Ru(bpy)(CH_3CN)_3Cl]\ [BF_4]$

Prolonged irradiation of the solution at 366 nm produces a new complex, $[Ru(bpy)(CH_3CN)_3Cl]^+$, as revealed by the slow emergence of an absorption band maximum at short wavelength ($\lambda_{max} = 436$ nm (3.94×10^3), *cf.* $[Ru(bpy)(CO)(CH_3CN)Cl_2]$ and $[Ru(bpy)(CH_3CN)_2Cl_2]$, isosbestic points at 467 and 341 nm).

It should be noted that $[Ru(bpy)(CH_3CN)_3Cl]^+$ is more rapidly built-up upon photolysis of a CH_3CN solution of $[Ru(bpy)(CO)_2Cl_2]$ or of its mono-photosubstituted form $[Ru(bpy)(CO)(CH_3CN)Cl_2]$ using a xenon lamp (sun lamp). In this situation $[Ru(bpy)(CH_3CN)_2Cl_2]$ is not transitory. This change in the selectivity of the photoprocess is probably due to the greater photoreactivity of $[Ru(bpy)(CO)(CH_3CN)Cl_2]$ under

visible irradiation since the MLCT absorption band of this complex is centred at 460 nm.

The identity of $[Ru(bpy)(CH_3CN)_3Cl]^+$ has been clearly established by mass spectroscopy analysis of the photolyzed solution after its evaporation to dryness. FAB^+ exhibits the expected molecular peak and characteristic fragmentation patterns: 415.9 $[M]^+$, 374.9 $[M-CH_3CN]$, 333.9 $[M-2CH_3CN]$, 292.9 $[M-3CH_3CN]$, 257.9 $[M-3CH_3CN-Cl]$. Moreover the IR spectrum reveals the lack of any CO band but the presence of a strong BF_4^- vibration at 1062 cm^{-1} and a ν(CN) stretching frequency at 2282 cm^{-1}. The CV of the photolyzed solution in CH_3CN + 0.06 M TMATF is shown in Fig. 2 (curve d). Two successive anodic waves are observed. The first quasi-reversible system ($Ep_a = 0.61$ V [9]) is due to Cl^- released during the photosubstitution, while the reversible more anodic system ($E_{1/2} = 0.73$ V) corresponds to the oxidation of $[Ru^{II}(bpy)(CH_3CN)_3Cl]^+$ into $[Ru^{III}(bpy)(CH_3CN)_3Cl]^{2+}$. As expected, the replacement of one Cl^- ligand by a poorer electron donor (CH_3CN) induces a shift of the $E_{1/2}$ of the $Ru^{2+/3+}$ process to a more anodic value. It is worth noting that the $E_{1/2}$ of the systems $[Ru(bpy)(CO)(CH_3CN)Cl_2]^{0/+}$ and $[Ru(bpy)(CH_3CN)_3Cl]^{+/2+}$ are close. The corresponding Ru^{3+} complex was produced by exhaustive controlled potential oxidation at 1.0 V. Two electrons per molecule of complex are consumed, one involving oxidation of Cl^- to Cl_2, which reacts irreversibly with acetonitrile [9] to give compounds which are not electroactive in the anodic region. After this electrolysis only the $[Ru(bpy)(CH_3CN)_3Cl]^{+/2+}$ couple is still present (Fig. 2). The absorption band of $[Ru(bpy)(CH_3CN)_3Cl]^{2+}$ lies at 454 nm (3.02×10^3) (Fig. 3(C), curve b) with a shoulder at 600 nm.

In the cathodic region a partially reversible system appears at $E_{1/2} = -1.88$ V for a solution of $[Ru(bpy)(CH_3CN)_3Cl]^+$, due to the ligand-centred reduction to $[Ru(bpy^{\cdot -})(CH_3CN)_3Cl]$. Confirmation of the instability of this species is obtained by exhaustive electrolysis carried out at −2.0 V. Only the Cl^-/Cl_2 system is then clearly detected on the CV of the electrolyzed solution.

2.2. *Photolysis of $[Me_4N]$ $[Ru(bpy)(CO)Cl_3]$*

Irradiation of a solution of $[Me_4N]$ $[Ru(bpy)(CO)Cl_3]$ (0.25×10^{-3} M) in CH_3CN at 366 nm or with a sun lamp induces rapid substitution of one chloro-ligand by CH_3CN leading to the quantitative formation of $[Ru(bpy)(CO)(CH_3CN)Cl_2]$. After a few minutes irradiation the solution exhibits an absorption spectrum ($\lambda_{max} = 460$ nm, Fig. 4(A), curve b) identical to that obtained following the first irradiation of a $[Ru(bpy)(CO)_2Cl_2]$ solution in CH_3CN. The quantum yield of the photoprocess is moderately high ($\Phi = 0.3$). The CV of the photolyzed solution recorded in CH_3CN + 0.06 M TMATF displays features of both the Cl^-/Cl_2 and $[Ru(bpy)(CO)(CH_3CN)Cl_2]^{0/+}$ redox system (Fig. 4b) in the anodic region and the irreversible reduction of $[Ru(bpy)(CO)(CH_3CN)Cl_2]$ in the cathodic region. Controlled-potential oxidation at 0.68 V eliminates the Cl^- ions, (Fig. 4(B)) and controlled-potential oxidation at 0.9 V results in the exhaustive formation of $[Ru^{III}(bpy)(CO)(CH_3CN)Cl_2]^+$. This species is identified by its typical visible absorption spectrum ($\lambda_{max} = 490$ nm (1.62×10^3), 406 nm ($2.02 \times$

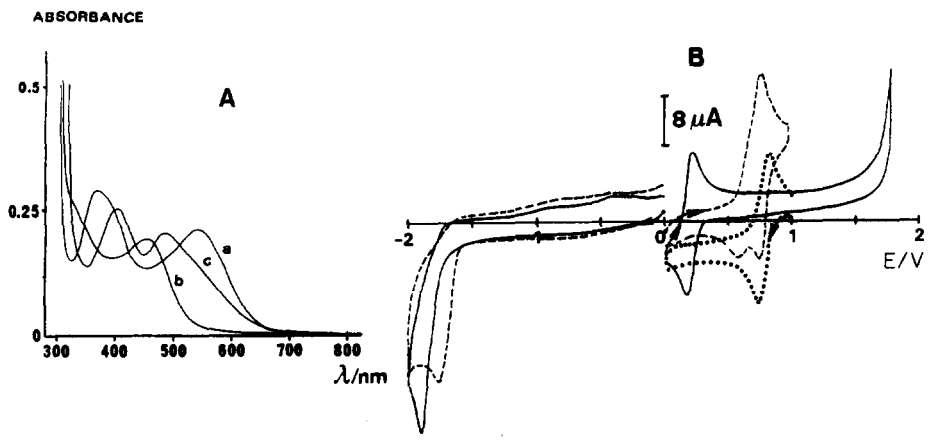

Fig. 4. (A) Spectral changes of a solution $[Me_4N][Ru(bpy)(CO)Cl_3]$ (0.25 mM) in CH_3CN + 0.06 M TMATF: (a) initial solution; (b) after photolysis with a 250 W xenon lamp; t = 4 mm; (c) after oxidation at 0.9 V; Q = 1 electron per molecule. (B) Cyclic voltammograms of a solution of 0.25 mM $[Me_4N][Ru(bpy)(CO)Cl_3]$ in CH_3CN + 0.06 M TMATF; sweeprate $\nu = 100$ mV s^{-1}. ——— initial solution; - - - - - - after photolysis with a 250 W Xe lamp; t = 4 mm; ····· after oxidation at 0.9 V; Q = 1 electron per molecule.

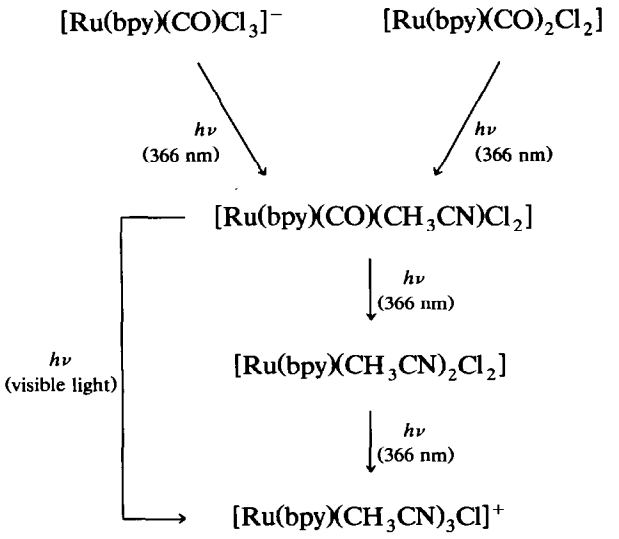

Scheme 1.

10^3), Fig. 4(A), spectrum c). Further photolyses at 366 nm of the solution of $[Ru(bpy)(CO)(CH_3CN)Cl_2]$ obtained under the conditions described above lead to the successive formation of $[Ru(bpy)(CH_3CN)_2Cl_2]$ and $[Ru(bpy)(CH_3CN)_3Cl]^+$. Scheme 1 summarizes the evolution of the complexes $[Ru(bpy)(CO)_2Cl_2]$ and $[Me_4N][Ru(bpy)(CO)Cl_3]$ under light irradiation in CH_3CN.

2.3. Photolysis of $[Ru(bpyest)(CO)_2Cl_2]$ (bpyest = 4,4'-di(isopropoxycarbonyl)-2,2'-bipyridine)

Photolysis of the above complex at 366 nm results in the successive and quantitative formation of $[Ru(bpyest)(CO)(CH_3CN)Cl_2]$ and $[Ru(bpyest)(CH_3CN)_2Cl_2]$. This is demonstrated by the changes in the absorption spectra and CV during the irradiation. Figure 5(A) shows the continuous build up of $[Ru(bpyest)(CO)(CH_3CN)Cl_2]$ (λ_{max} = 508 nm (3.04×10^3), 381 nm (4.61×10^3). During the course of the photolysis, successive UV visible spectra generate a series of isosbestic points (λ = 339, 324, 294 and 271 nm). The quantum yield of the photoreaction is quantitative, as with the complex containing the unsubstituted bpy ligand. FAB$^+$ 569.0 $[M + H]^+$, 528.0 $[M + H-CH_3CN]$, 500.0 $[M + H-CH_3CN-CO]$ and IR spectroscopy (only one ν(CO) band at 1970 cm^{-1}, ν(ester) at 1724 cm^{-1} and ν(CN) at 2283 cm^{-1}) confirms the identity of the $[Ru(bpyest)(CO)(CH_3CN)Cl_2]$ species.

The reversible one-electron oxidation of this new complex is located at $E_{1/2}$ = 0.85 V (Fig. 6, curve b). The cathodic shift of the $Ru^{II/III}$ system compared to that of the initial complex ($E_{1/2}$ = 1.50 V; Fig. 6 curve a) is similar to that observed for $[Ru(bpy)(CO)_2Cl_2]$. Exhaustive electrolysis at 0.95 V gives the stable Ru^{III} species $[Ru^{III}(bpyest)(CO)(CH_3CN)Cl_2]^+$ (λ_{max} = 547 nm, sh, 497 nm (2.06×10^3), 407 nm (3.06×10^3)). The CV in the cathodic region shows that the ligand-based reduction system $[Ru(bpyest)(CO)(CH_3CN)Cl_2]/[Ru(bpyest^{\cdot-})(CO)(CH_3CN)Cl_2]^-$ is reversible ($E_{1/2}$ = −1.42 V). These results are consistent with the stabilizing electronic effect of the electron-withdrawing bpyest. However, bulk electrolysis at −1.55 V reveals that $[Ru(bpyest^{\cdot-})(CO)(CH_3CN)Cl_2]^-$ is unstable and that 2 Cl^- per molecule of complex are liberated. The reversible couple is accompanied by an irreversible peak at Ep_c = −1.73 V.

Figure 5B depicts the formation of $[Ru(bpyest)(CH_3CN)_2Cl_2]$. Its absorption bands are located at λ_{max} = 598 nm (6.57×10^3), 455 nm (1.2×10^4) and the corresponding isosbestic points at λ = 391, 321, 311 and 270 nm. The quantum yield of the transformation is quite low (Φ = 0.02). IR (no ν(CO), ν(ester) = 1716 cm^{-1} and ν(CN) at 2274 cm^{-1}) and FAB$^+$ spectroscopic 581.8 [M], 540.8 $[M-CH_3CN]$, 505.8 [M-

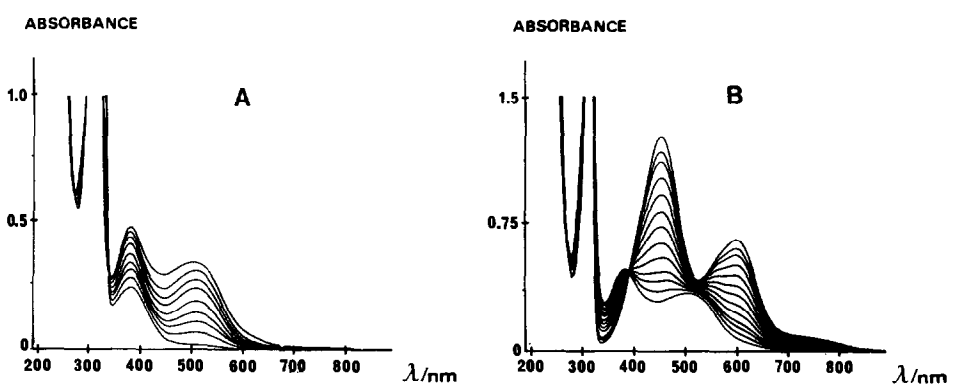

Fig. 5. Spectral changes during irradiation with a 250 W mercury lamp at 366 nm of a solution $[Ru(bpyest)(CO)_2Cl_2]$ (1.0 mM) in CH_3CN. (A) Formation of $[Ru(bpyest)(CO)(CH_3CN)Cl_2]$: (a) t = 0 s; (i) t = 12 min 30 s. (B) Formation of $[Ru(bpyest)(CH_3CN)_2Cl_2]$: (a) t = 12 min 30 s, (m) t = 10 h 10 min.

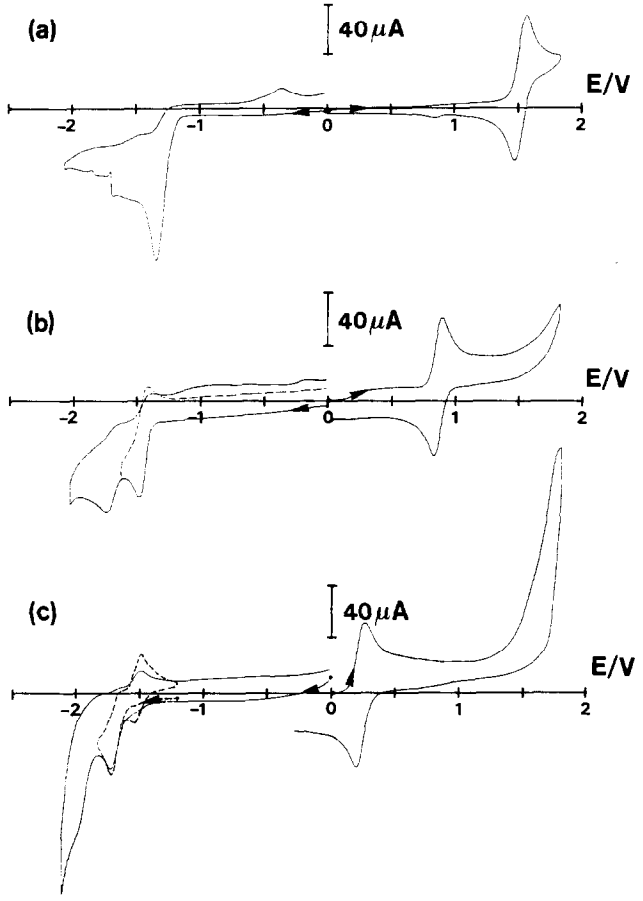

Fig. 6. Cyclic voltammograms of a solution of $[Ru(bpyest)(CO)_2Cl_2]$ in CH_3CN + 0.06 M TMATF: (a) initial solution (1.0×10^{-3} M); (b) after formation of $[Ru(bpyest)(CO)(CH_3CN)Cl_2]$ (1.0×10^{-3} M); (c) after formation of $[Ru(bpyest)(CH_3CN)_2Cl_2]$ (0.9×10^{-3} M).

$CH_3CN-Cl]$, 499.8 $[M-2CH_3CN]$, 464.8 $[M-2CH_3CN-Cl]$ analysis confirms the structure of the complex. Only one reversible anodic $Ru^{2+/3+}$ system ($E_{1/2} = 0.22$ V) is observed in the CV (Fig. 6, curve c) demonstrating that the photosubstitution is quantitative. The corresponding stable $[Ru^{III}(bpyest)(CH_3CN)_2Cl_2]^+$ complex is obtained upon controlled-potential oxidation at 0.6 V, after the consumption of one electron per mole. Its UV visible spectrum ($\lambda_{max} = 427$ nm (9.1×10^3), 390 nm, sh) is close to that calculated for $[Ru^{III}(bpy)(CH_3CN)_2Cl_2]^+$. No ruthenium–carbonyl band is detected in the IR spectrum (ν(ester) = 1722 cm^{-1}, ν(CN) = 2300 cm^{-1}) while the expected molecular and fragmentation peaks 581.8 $[M]^+$, 540.9 $[M-CH_3CN]$, 499.9 $[M-2CH_3CN]$, 464.9 $[M-2CH_3CN-Cl]$ are observed on the FAB^+ spectrum.

The reductive pattern of $[Ru(bpyest)(CH_3CN)_2Cl_2]$ suggests a slightly reversible process at $E_{1/2} = -1.66$ V followed by an irreversible one at $Ep_c = -1.97$ V. Furthermore two successive scans recorded between -1.20 V and -1.80 V shows that the first reduction process induces the emergence of a reversible system at $E_{1/2} = -1.49$ V (see Fig. 6, curve c). No attempt was made to determine the nature of this system.

The tris(CH_3CN)-substituted complex cannot be obtained by prolonged photolysis at 366 nm. However slow partial formation of $[Ru(bpyest)(CH_3CN)_3-Cl]^+$ can be observed in prolonged irradiation with a sunlight lamp. A maximum yield of $[Ru(bpyest)(CH_3CN)_3-Cl]^+$ of 25% was obtained. This was revealed by the examination of the absorption spectrum and CV after photolysis. Shoulders appear in the range 320–400 nm and evidence of a partially reversible system at $E_{1/2} = 0.82$ V.

2.4. *Photolysis of $[Me_4N][Ru(bpyest)(CO)Cl_3]$*

The expected photosubstitution of the complex into $[Ru(bpyest)(CO)(CH_3CN)Cl_2]$ is only efficient under irradiation with a sun lamp or a selective photolysis at 436 nm. The quantum yield at this wavelength is 0.06. Further irradiation at 366 nm leads to the slow and quantitative formation of $[Ru(bpyest)(CH_3CN)_2Cl_2]$, as with $[Ru(bpyest)(CO)_2Cl_2]$.

3. Discussion

The photophysical properties of all these new complexes have not yet been studied in detail, consequently the mechanisms of the photosubstitution processes are not precisely known. However, in the light of detailed studies carried out on related complexes, we postulate that photoinduced CO release is a common phenomenon for metal carbonyl complexes, attributed to metal-centred *d–d* excited states [10]. The relatively low photoreactivity of the monocarbonyl-ruthenium(II) complexes compared to the high photoreactivity of the dicarbonylruthenium(II) complexes, is consistent with a metal-to-ligand charge-transfer excited state located at lower energy than the reactive (probably triplet) d–d excited states. Analogous observations have been made in a bisbipyridinemonocarbonyl ruthenium(II) series of complexes [11].

4. Conclusion

The present work shows that the $[Ru^{II}(L)(CO)_2Cl_2]$ and $[Me_4N][Ru^{II}(L)(CO)Cl_3]$ undergo facile successive photosubstitutions in acetonitrile and presumably in other coordinating organic solvents. The selectivity of the photosubstitution can be controlled with particular wavelengths of irradiation. Several new complexes have been prepared in this way. The replacement of the bpy ligand by electron-withdrawing carboxy-ester groups slows down the photosubstitutions. It allows the quantitative formation of the disubstituted complex

$[Ru(L)(CH_3CN)_2Cl_2]$ since the subsequent reaction to $[Ru(L)(CH_3CN)_3Cl]^+$ is inefficient.

5. Experimental

5.1. Material

5.1.1. General procedure for the preparation of $[Ru(L)(CO)_2Cl_2]$

Polymeric dicarbonyldichlororuthenium (ruthenium red carbonyl) solutions were prepared by an adaptation of a literature method [12]. In a 100 ml three-necked flask, 1 g of $RuCl_3 \cdot 3H_2O$ (3.82 mmole, 1 equiv.) dissolved in 70 ml ethanol were heated under reflux for 7 h under a continuous flow of carbon monoxide. After cooling to *ca.* 40°C under carbon monoxide, 3.82 mmole (1 equiv.) of the solid bidentate ligand were added. After heating the solution with reflux for two additional hours under argon and cooling to room temperature, the brick-red crystalline solid was filtered, washed with cold ethanol and ether, and dried under high vacuum. The red solid consisted of a mixture of $[Ru^{II}(bpy)(CO)_2Cl_2]$ and $[Ru^{III}(bpy)(CO)Cl_3]$ (80% yield).

$[Ru^{II}(bpy)(CO)_2Cl_2]$ was isolated as follows: 1.5 g of the mixture was dissolved in a 200 ml ethanol/water mixture (1:1) and heated under reflux under argon for 2 h (1/3 of the volume of acetonitrile was used in the case of the 4,4'-substituted-bpy). During reflux, the colour of the solution changed from red to yellow. After cooling to room temperature, the solution was evaporated to half volume, resulting in the precipitation of a pale yellow solid. The pure complex was collected by centrifugation, washed with water/ethanol (1:1) and finally with diethyl ether. A 37% yield was obtained after drying under high vacuum.

5.1.2. Characterization of $[Ru(bpy)(CO)_2Cl_2]$

^1H NMR (acetonitrile-d_3): δ 9.19 (d, 2H-6,6', $^3J_{6-5}$ 8.1 Hz), 8.47 (d, 2H-3,3', $^3J_{3-4}$ 8 Hz), 8.24 (td, 2H-4,4', $^3J_{4-3}$ and $^3J_{4-5}$ 8.1 Hz, $^4J_{4-6}$ 1.5 Hz), 7.76 (td, 2H-5,5', $^3J_{5-6}$ and $^3J_{5-4}$ 8.1 Hz, $^4J_{5-3}$ 1.5 Hz). $^{13}C\{^1H\}$ (acetonitrile-d_3): δ 197.38 (Ru–CO), 155.55 (CC, bpy) 153.84, 141.28, 128.73, 124.98 (CH, bpy).

FAB^+ (*m*-NBA): 383.9 $[M+H]^+$, 355.8 [M + H + CO], 349.0 [M + H–Cl], 327.9 [M + H–2CO], 321.0 [M + H–Cl–CO], 292.9 [M + H–2CO–Cl], 257.0 [M–2CO–2Cl]. UV-Vis λ_{max}, nm (ϵ: l mol^{-1} cm^{-1}): 352 (1.55×10^3), 313 (1.41×10^4), 300 (1.13×10^4), 286 (1×10^4), 246 (9.6×10^3).

IR (Nujol mull): 2055 cm^{-1} (vs, ν(Ru–CO)), 1995 (vs, ν(Ru–CO)), 1600 (m), 1305 (m), 1245 (ω), 765 (s).

Anal. Found.: C, 37.32; H. 2.08; N, 7.17; Cl, 18.21. $C_{12}H_8Cl_2N_2O_2Ru$ calcd.: C, 37.51; H, 2.10; N, 7.29; Cl, 18.46%.

5.1.3. Characterization of $[Ru(bpyest)(CO)_2Cl_2]$

^1H NMR (acetonitrile-d_3): δ 9.35 (d, 2H-6,6', $^3J_{6-5}$ 5.7 Hz), 8.97 (d, 2H-3,3', $^3J_{3-5}$ 1.6 Hz), 8.18 (dd, 2H-5,5', $^3J_{5-6}$ 5.7 Hz and $^4J_{5-3}$ 1.6 Hz), 5.32 (h, 2H (CH), ^3J 6.2 Hz), 1.43 (d, 12H (CH_3), ^3J 6.2 Hz). $^{13}C\{^1H\}$ (acetonitrile-d_3): δ 196.87 (Ru–CO), 163.3, 155.90, 154.89 (CH (of bidentate ligand)), 142.97, 127.84 and 124.53 (3CH (of bidentate ligand)), 71.90 (CH (of ^{i}Pr)), 21.85 (CH_3).

FAB^+ (*m*-NBA): 555.9 $[M+H]^+$, 527.9 [M + H–CO], 520.9 [M + H–Cl], 499.9 [M + H–2CO], 492.3 [M + H–Cl–CO], 464.9 [M + H–Cl–2CO].

UV-Vis λ_{max}, nm (ϵ; 1 mol^{-1} cm^{-1}): 383 (2.1×10^3), 329.2 (1.19×10^4), 315.2 (1.3×10^4), 235.8 (2.7×10^4).

IR (Nujol mull): 2060 cm^{-1} (vs, ν(Ru–CO)), 1995 (vs, ν(Ru–CO)), 1718 (vs, ν(ester)), 1560 (m), 1270 (s), 1230 (s), 1105 (vs), 765 (s).

Anal. Found: C, 42.89; H, 3.40; N, 4.91; Cl, 12.49. $C_{20}H_{20}Cl_2N_2O_6Ru$ calcd.: C, 43.17; H, 3.62; N, 5.04; Cl, 12.75%.

$[Me_4N][Ru(L)(CO)Cl_3]$ was synthesized from the crude red-brick crystalline solid obtained during the preparation of $[Ru(L)(CO)_2Cl_2]$ following an electrochemical procedure reported earlier [6]. Typically, exhaustive reduction of 34.2 mg of the red compound at -1.65 V in CH_3CN + 0.06 M TMATF gave 8.3 mg of $[Me_4N][Ru^{II}(bpy)(CO)Cl_3]$ as a bright red precipitate. A similar synthetic procedure was used to prepare $[Me_4N][Ru^{II}(bpyest)(CO)Cl_3]$, except that for this complex evaporation of the solvent after electrolysis was needed since it is soluble in CH_3CN. The residue was then extracted twice with CH_2Cl_2 and the solid obtained after removal of CH_2Cl_2 dried under vacuum.

$[Me_4N][Ru(bpy)(CO)Cl_3]$: FAB^- (m-NBA): 392.9 $[M]^-$, 357.0 [M–Cl]. UV-Vis (CH_3CN) λ_{max}, nm (ϵ; l mol^{-1} cm^{-1}); 546 (1.94×10^3), 372 (2.62×10^3). IR (CD_2Cl_2): 1925 cm^{-1} (vs, ν(Ru–CO)), 1485 (s, $\nu(Me_4N^+)$), 950 (s, $\nu(Me_4N^+)$).

$[Me_4N][Ru(bpyest)(CO)Cl_3]$: FAB^- (m-NBA): 564.9 $[M]^-$, 536.9 [M–CO], 499.9 [M–CO–Cl]. UV-Vis (CH_3CN) λ_{max}, nm (ϵ; 1 mol^{-1} cm^{-1}) 615 (2.47×10^3), 437 (4.40×10^3). IR (CD_2Cl_2): 1940 cm^{-1} (vs. ν(Ru–CO)), 1725 (vs, ν(ester)), 1485 (m, $\nu(Me_4N^+)$).

The 2,2'-bipyridine was purchased from Aldrich and the bpyest was prepared following the method reported in the literature [13].

Acetonitrile (Rathburn, HPLC grade) was dried by distillation from P_2O_5. CH_2Cl_2 was dried by passage through an alumina column. Tetramethylammonium tetrafluoroborate (TMATF) (Fluka) was washed with

an excess of warm CH_2Cl_2, and dried under vacuum at 80°C for three days.

5.2. Spectra and analysis

All electronic spectra were recorded on a Cary 1 spectrophotometer for experiments run without an argon purge, or on a Hewlett Packard 8452A diode array spectrophotometer for experiments (essentially electrochemical experiments) conducted in a dry box under argon. The photolyzed and electrolyzed solutions were transferred to a conventional cuvette cell in the dry box. The cell was inserted in an optical translater connected in the spectrophotometer through a fibre optic system (Photonetics Spectrofip system).

Fast Atom Bombardment mass spectra (FAB) were obtained on an AEI Kratos MS 50 spectrometer fitted with an Ion Tech Ltd. gun (Centre de Recherche sur les Macromolécules Végétales, Grenoble) or on a SAB-HF-VG Analytical Apparatus (Ecole Européenne des Hautes Etudes des Industries Chimiques de Strasbourg) using *meta*-nitrobenzyl alcohol (*m*-NBA) as matrix.

Infrared spectra were recorded on a Bruker FTIR IFS 25 spectrometer. ^1H and ^{13}C NMR spectra were recorded on a Bruker SY-200 spectrometer at 200.1 MHz (^1H) and 50.3 MHz (^{13}C), with the solvent as an internal standard.

5.3. Photolysis systems

For the determination of the quantum yield at 366 and 436 nm, the desired mercury emission line from a 250 W mercury lamp (Applied Photophysics type ME/D) was selected by using a band-pass filter (Oriel model 5653 and 5655). Light intensities absorbed by the samples were measured as previously reported [14]. Quantum yield determinations were carried out spectrophotometrically at the maximum wavelength of the absorption of $[Ru(L)(CO)(CH_3CN)Cl_2]$, $[Ru(L)(CH_3CN)_2Cl_2]$, and $[Me_4N][Ru(L)(CO)Cl_3]$ by comparing the absorption of the sample before and after irradiation. The photolysis cell was an optical cuvette of 1 mm pathlength for continuous spectrophotochemical experiments and a 2 or 5 cm pathlength cell for electrochemical experiments. For the latter, the solution was purged with argon prior to introduction to the dry box and then transferred to a conventional three-electrode electrochemical cell. Irradiations were run in CH_3CN. The presence or absence of supporting electrolyte (TMATF), did not affect the result. Irradiations with a sun lamp were made with an Osram 250 W xenon lamp equipped with T_2 and T_{a2} MTO filters to exclude IR wavelengths.

5.4. Electrochemical instrumentation

Electrochemical experiments were carried out with a Princeton Applied Research Model 273 Potentiostat Galvanostat equipped with a Sefram TGM 164 X–Y recorder. The working electrode was a Pt disk (5 mm diameter) polished with a 1 μm diamond paste. All potentials are relative to the Ag/Ag^+ couple (10 mM) + 0.06 M TMATF in CH_3CN as electrode. All experiments were run under an argon atmosphere in a dry box (Jaram).

References

1 See for example: J. R. Pugh, M. R. M. Bruce, B. P. Sullivan and T. J. Meyer, *Inorg. Chem., 30* (1991) 86.
2 J.-M. Lehn and R. Ziessel, *J. Organomet. Chem., 383* (1990) 157.
3 M. Ishida, K. Fujiki, T. Omba, K. Ohkubo, K. Tanaka, T. Terada and T. Tanaka, *J. Chem. Soc., Dalton Trans.*, (1990) 2155.
4 J. Chatt, B. L. Shaw and A. E. Field, *J. Chem. Soc.*, (1964) 3466; S. O. Robinson and G. Wilkinson, *J. Chem. Soc. A*, (1966) 300.
5 J. M. Kelly, C. M. O'Connell and J. G. Vos, *Inorg. Chim. Acta, 64* (1982) L75.
6 M.-N. Collomb-Dunand-Sauthier, A. Deronzier and R. Ziessel, *J. Electroanal. Chem., 319* (1991) 347.
7 S. Cosnier, A. Deronzier and J.-C. Moutet, *New J. Chem., 14* (1990) 831.
8 G. Denti, L. Sabatino, G. De Rosa, A. Bartolotta, G. Di Marco, V. Ricevuto and S. Campagna, *Inorg. Chem., 28* (1989) 3309 and references therein.
9 G. Cauquis, A. Deronzier, B. Sillon, B. Damin and J. Garapon, *J. Electroanal. Chem., 117* (1981) 139 and references therein.
10 G. L. Geoffroy and M. S. Wrighton, in *Organometallic Photochemistry*, Wiley, New York, 1979.
11 J. M. Kelly, C. O'Connell and J. G. Vos, *J. Chem. Soc., Dalton Trans.*, (1986) 253.
12 M. J. Cleave and W. P. Griffiths, *J. Chem. Soc. A*, (1969) 372.
13 P. J. Delaive, J. T. Lee, H. W. Sprintschnik, M. Abruña, T. J. Meyer and D. G. Whitten, *J. Am. Chem. Soc., 99* (1977) 7094.
14 A. Deronzier and F. Esposito, *Nouv. J. Chim., 7* (1983) 15.